Southeast-Asian J. of Sciences: Vol. 2, No 1 (2013) pp. 19-26

NUMERICAL SIMULATION OF SELF-PROPELLED MOTION OF TWO ROTATING SIDE-BY-SIDE CIRCULAR CYLINDERS

Pairin Suwannasri

Department of Mathematics Statistics and Computer
Ubon Ratchathani University
Ubon Ratchathani 34190, Thailand
C. of Excellence in Math., Bangkok 10400, Thailand
e-mail: scpuirsu@ubu.ac.th

Abstract

In the present work, the problem of the motion of self-propelled two rotating side-by-side circular cylinders in a viscous incompressible fluid is investigated numerically. The surface of left cylinder rotates counter-clockwise and right clockwise at the same speed. The flow patterns and the drag coefficients of regimes of self-motion are analyzed for a various range of rotational speed and different gap spacings at a moderate Reynolds number.

1 Introduction

In physical and biological sciences, and in engineering, there is a wide range of problems of interest concerning the flow past a self-propelled bodies. The propulsion may be by means of drawing fluid inwards across portions of the boundary and expelling it from others, so that the net flux of momentum across the boundary is nonzero. The literature on the numerical simulation of motion of self-propulsion of a rotating body has not been investigated widely. There is only Sungnul and Moshkin (2006) studied the self-propelled motion of two rotating circular cylinders. They found that a self-motion regime occur at

Key words: two rotating circular cylinders, self-propelled motion.

critical rotational speed of the surface of left cylinder rotates clockwise and right counter-clockwise.

In this work, we extend on the more limited work by Sungnul and Moshkin. We examine the the problem of the motion of self-propelled two rotating circular cylinders in more detail and consider the case of the surface of left cylinder rotates counter-clockwise and right clockwise at the same speed.

2 Mathematical model

Assuming the flow remains axisymmetric for all time, makes the cylindrical bipolar coordinate system attached to the cylinder:

$$x = \frac{c\sinh\eta}{\cosh\eta - \cos\xi}, \quad y = \frac{c\sin\xi}{\cosh\eta - \cos\xi}, \quad z = z, \tag{1}$$

where $\xi \in [0, 2\pi)$, $\eta \in (-\infty, \infty)$, $z \in (-\infty, \infty)$, c is a characteristic length which is positive. The curves of constant ξ and η are circles in xy-space

$$x^2 + (y - c\cot\xi)^2 = c^2\csc^2\xi, \;\; (x - c\coth\eta)^2 + y^2 = c^2\mathrm{csch}^2\eta. \tag{2}$$

Figure 1 shows the two cylinders have diameter D and the distance between them is g. If g and D are given, one can find c and η as following

$$c = \frac{D}{2}\sqrt{g^{*2} + 2g^*}, \quad \eta = \ln\left((g^* + 1) \pm \sqrt{(g^* + 1)^2 - 1}\right), \text{ as } \quad g^* = \frac{g}{D}.$$

The Navier-Stokes equations in the cylindrical bipolar coordinate system (ξ, η, z) are

$$\frac{\partial v_\xi}{\partial t} + \frac{1}{h}\left(v_\xi\frac{\partial v_\xi}{\partial \xi} + v_\eta\frac{\partial v_\xi}{\partial \eta}\right) - \frac{1}{c}\left(\sinh\eta(v_\xi v_\eta) - \sin\xi(v_\eta)^2\right) = -\frac{1}{h}\frac{\partial p}{\partial \xi}$$
$$+\frac{2}{Re}\left[\frac{1}{h^2}\left(\frac{\partial^2 v_\xi}{\partial \xi^2} + \frac{\partial^2 v_\xi}{\partial \eta^2}\right) - \frac{2}{ch}\left(\sinh\eta\frac{\partial v_\eta}{\partial \xi} - \sin\xi\frac{\partial v_\eta}{\partial \eta}\right) - \left(\frac{\cosh\eta + \cos\xi}{c}\right)v_\xi\right], \tag{3}$$

$$\frac{\partial v_\eta}{\partial t} + \frac{1}{h}\left(v_\xi\frac{\partial v_\eta}{\partial \xi} + v_\eta\frac{\partial v_\eta}{\partial \eta}\right) + \frac{1}{a}\left(\sinh\eta(v_\xi)^2 - \sin\xi(v_\xi v_\eta)\right) = -\frac{1}{h}\frac{\partial p}{\partial \eta} \tag{4}$$
$$+\frac{2}{Re}\left[\frac{1}{h^2}\left(\frac{\partial^2 v_\eta}{\partial \xi^2} + \frac{\partial^2 v_\eta}{\partial \eta^2}\right) + \frac{2}{ch}\left(\sinh\eta\frac{\partial v_\xi}{\partial \xi} - \sin\xi\frac{\partial v_\xi}{\partial \eta}\right) - \left(\frac{\cosh\eta + \cos\xi}{c}\right)v_\eta\right],$$

$$\frac{1}{h^2}\left[\frac{\partial(hv_\xi)}{\partial \xi} + \frac{\partial(hv_\eta)}{\partial \eta}\right] = 0, \tag{5}$$

where p is the pressure, v_ξ and v_η are the velocity components in ξ and η directions, respectively, and $h = c/(\cosh\eta - \cos\xi)$. The velocities are non dimensionalized with the free stream velocity U_∞, all lengths are non dimensionalized with the radius a and the pressure by ρU_∞^2. Here Re denotes the

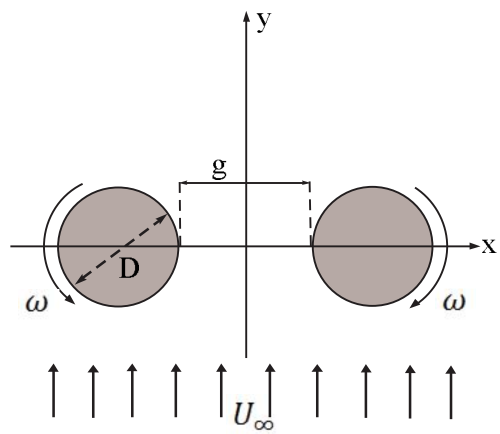

Figure 1: Sketch of the geometry of the problem.

Reynolds number defined by $Re = \dfrac{2U_\infty a}{\nu}$, where ν is the kinematic viscosity coefficient. Boundary conditions for v_ξ and v_η include the no-slip and impermeability conditions

$$v_\xi = \alpha, \quad v_\eta = 0, \quad \xi \in (0, 2\pi], \tag{6}$$

where $\alpha = (a\omega)/U_\infty$ is the nondimensional rotational velocity at the surface, the periodicity conditions

$$v_\xi\left(\xi,\eta\right) = v_\xi\left(\xi+2\pi,\eta\right), \; v_\eta\left(\xi,\eta\right) = v_\eta\left(\xi+2\pi,\eta\right), \; p\left(\xi,\eta\right) = p\left(\xi+2\pi,\eta\right), \tag{7}$$

and the far-field condition

$$\vec{v} = (v_x, v_y) = (0,1)\,, \quad p = \frac{p_\infty}{\rho U_\infty^2} \;\text{ as }\; x^2+y^2 \to \infty. \tag{8}$$

Here, v_x and v_y are the components of the velocity vector in the cylindrical coordinate system with

$$\begin{aligned} v_\xi &= \left(-\frac{h}{a}\sinh\eta\sin\xi\right)v_x + \left(\frac{h}{a}\left(\cosh\eta\cos\xi - 1\right)\right)v_y \\ v_\eta &= \left(-\frac{h}{a}\left(\cosh\eta\cos\xi - 1\right)\right)v_x - \left(\frac{h}{a}\sinh\eta\sin\xi\right)v_y. \end{aligned} \tag{9}$$

The main characteristic of the flow around the body is the drag coefficient which comprises a pressure drag coefficient and a viscous drag coefficient, *i.e.*

$C_D = C_{D_p} + C_{D_f}$. They are defined as

$$C_{D_p} = -\frac{1}{\rho U_\infty^2 D}\int\limits_{\Sigma} p\vec{n}\cdot\vec{i}_y dS, \quad C_{D_f} = -\frac{1}{\pi\rho U_\infty^2 D}\int\limits_{\Sigma} \mu\left(\vec{n}\times\vec{\omega}\right)\cdot\vec{i}_y dS$$

3 Numerical Method

In the case of steady flow, time in Equations (3) - (5) can be considered as an artificial (iterative) parameter. A staggered arrangement of the variables on a uniform grid is used. A two-step time-split projection method is utilized to advance the flow field. First, the velocity components are advanced from time level "n" to an intermediate level "*" by solving Equations (3) - (5) explicitly without the pressure term. In the advection-diffusion step, the spatial derivatives are approximated by the central finite differences. One side finite differences are utilized near boundaries due to the staggered arrangement of variables. Then the Poisson equation for the pressure is solved fully implicitly by the method of stabilizing correction (see Yanenko [7]). The equation for pressure is derived by using the mass conservation requirement for each computational cell. Once the pressure is updated, the final level is computed with a pressure-correction step. Figure 2 shows the computational domain, sketch of the grid, and location of the unknowns. Far-field boundary conditions (8) are shifted on the boundary of domains Ω_1 and Ω_2 which are defined as

$$\begin{aligned} &\Omega_1 = \{(\xi,\eta) \mid \ 0 \le \xi \le \varepsilon_\xi, -\varepsilon_\eta \le \eta \le \varepsilon_\eta\}, \\ &\Omega_2 = \{(\xi,\eta) \mid \ 2\pi - \varepsilon_\xi \le \xi \le 2\pi, -\varepsilon_\eta \le \eta \le \varepsilon_\eta\}, \end{aligned} \tag{10}$$

where $\varepsilon_\eta = K\triangle_\eta$ and $\varepsilon_\xi = M\triangle_\xi$, K and M are integer numbers, and $\triangle_\eta$ and $\triangle_\xi$ are the size of computational cell in the η and ξ directions, respectively. In the physical space (x, y, z) the boundaries of domains Ω_1 and Ω_2 are located sufficiently far from the cylinders and these boundaries are the coordinate surfaces that are convenient for the implementation of a finite difference method.

4 Results

The characteristics of flow past two rotating circular cylinders in side-by-side arrangement at Reynolds numbers $Re = 40$ with a rate of rotation of $-6.0 \le \alpha \le 3.0$ for $g^* = 1$ were studied. The cylinder is placed in a vertical stream (from down to up) of uniform flow velocity U_∞ as shown in Figure 1. Figure 3 demonstrates variation of toatla drag coefficient C_D versus rotation rate α for Reynolds numbers $Re = 40$ and $g^* = 1$. The graphics of $C_D = C_D(\alpha)$ have a bell shape with maximum value at $\alpha \approx -1.5$. The cases of zero drag correspond

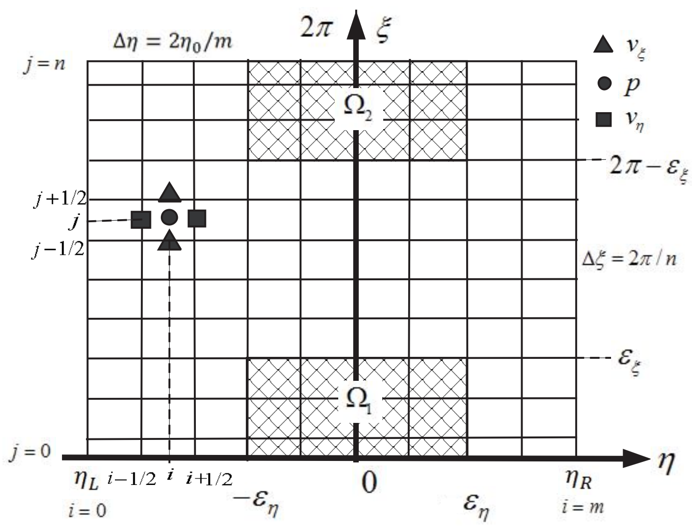

Figure 2: Staggered arrangement of u,v and p.

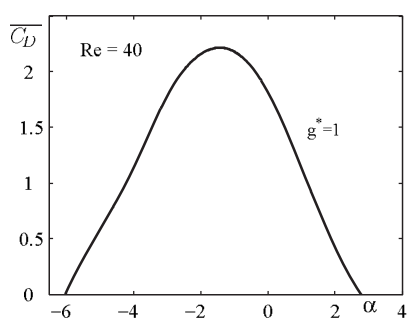

Figure 3: Variation of drag coefficient with rate of rotation for $Re = 40$ and $g^* = 1$.

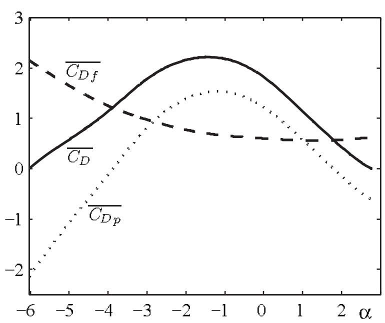

Figure 4: Pressure and firictional contributions to $C_D = C_{Dp} + C_{Df}$ for $Re = 40$ and $g^* = 1$.

to the self-motion of two rotating circular cylinders at $\alpha = -6.03$ and $\alpha = 2.79$. Figure 4 shows the pressure and viscous drag coefficient contributions to the total drag coefficient for Reynolds number $Re = 40$ and a gap spacing $g^* = 1$. Nonmonotonic behavior of C_D occurs due to variation of the pressure force. Figure 5 shows streamline pattern and direction of velocity vector for the case of $g* = 1$, $Re = 40$ and $\alpha = -6.03$ (self-motion), -5.0, -4.0, -2.0, 0.0, 1.0, 2.0 and 2.79 (self motion). In the self-motion regime corresponding to the positive α, the main stream flows around a virtual elliptic region which encloses the rigid cylinders.

The self-motion regime corresponding to the negative $\alpha \approx = -6.03$ associated with the jet of fluid expelled from the hole.

5 Conclusion

In the present study, we have investigated numerically the self-propelled of two rotating side-by-side circular cylinders at Reynolds number Re=40 with a gap spacing $g^* = 1$ for a range of rotational rate $-6.0 \leq \alpha \leq 3.0$. The self-propelled motions of two rotating circular cylinders occur at $\alpha = -6.03$ and $\alpha = 2.79$. Two regimes of self motion are difference. In the self-motion regime corresponding to the positive α, the main stream flows around a virtual elliptic region which encloses the rigid cylinders. The self-motion regime corresponding to the negative α associated with the jet of fluid expelled from the hole.

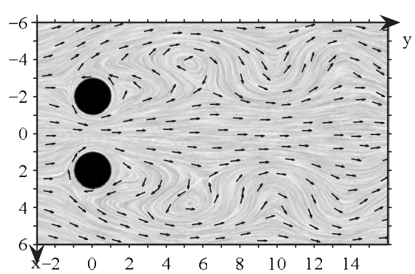

(c) $\alpha = -2.0$

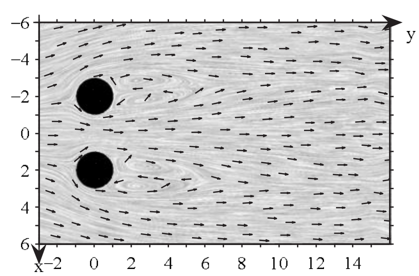

(g) $\alpha = 0.0$

References

[1] A.S. Chan, P.A. Dewey, A. Jameson, C. Liang and A.J. Smits, *Vortex suppression and drag reduction in the wake of counter-rotating cylinders*, J.Fluid Mech., 679 (2011), 343–382.

[2] S. Kang, *Chracteristics of flow over two circular cylinders in a side-by-side arrangement at low Reynolds numbers*, Phys, Fluids, 15 (2003), 2486–2498.

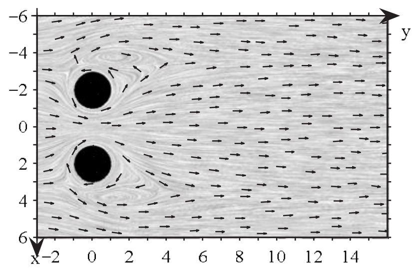

(*c*) $\alpha = -4.0$

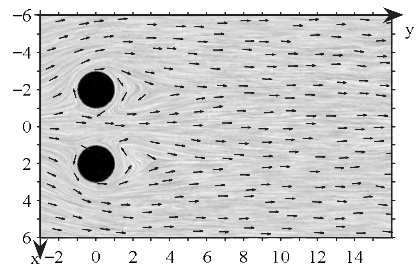

(*g*) $\alpha = 1.0$

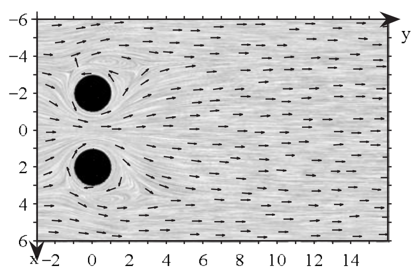

(*c*) $\alpha = -5.0$

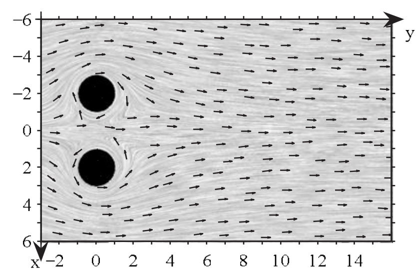

(*g*) $\alpha = 2.0$

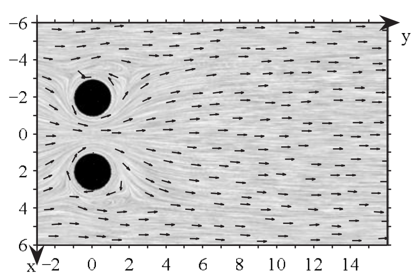

(*d*) $\alpha = -6.03$(self-motion: $C_D = 0$)

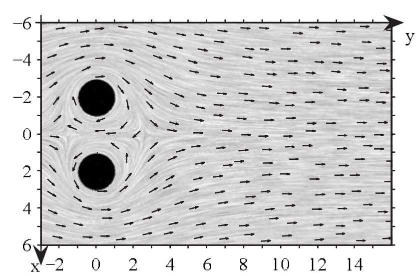

(*f*) $\alpha = 2.79$(self-motion: $C_D = 0$)

Figure 5: Streamline patterns of flow past two rotating circular cylinders at $Re = 40$ with $g* = 1$.

[3] H. Nemati, K. Sedighi, M. Farhadi, M.M. Pirouz and E. Fattahi, *Numerical simulation of fluid flow of two rotating side-by-side circular cylinders by Lattice Boltzmann method*, J.Fluid Mech., 495 (2003), 255–281.

[4] N.P. Moshkin,and P. Suwannasri, *Self-propelled motion of a torus rotating about its centerline in a viscous incompressible fluid*, Phys. Fluids, 22 (2010), 113602.

[5] N.P. Moshkin,and P. Suwannasri, *Two regimes of self-propelled motion of a torus rotating about its centerline in a viscous incompressible fluid at intermediate Reynolds numbers*, Phys. Fluids, 24 (2012), 053603.

[6] S. Sungnul and N.P. Moshkin, *Numerical simulation of steady viscous flow past two rotating circular cylinders*, Suranaree J. Sci. Technol., 13(3) (2006), 219–233 .

[7] N.N. Yanenko, *The method of Fractional Steps: The Solution of Problems of Mathematical Physics in Several Variables*, New York, Springer-Verlag (1971).